# MODE IDENTIFICATION OF BPM 37093 WITH THE HST

A. Nitta<sup>1</sup>, A. Kanaan<sup>2</sup>, S. O. Kepler<sup>3</sup>, D. Koester<sup>4</sup>, M. H. Montgomery<sup>5</sup> and D. E. Winget<sup>1</sup>

<sup>1</sup> Astronomy Department, University of Texas, TX 78712, Austin, U.S.A.

<sup>2</sup> Instituto de Física, Universidade Federal de Santa Catarina, CP 476, CEP 88040-900, Florianópolis, Brazil

<sup>3</sup> Instituto de Física, Universidade Federal do Rio Grande do Sul, Campus do Vale, CP 15051 Goncalves, Porto Alegre, Brazil

<sup>4</sup> Institut für Theoretische Physik und Astrophysik, Universität Kiel, D-24098 Kiel, Germany

Institut f\(\tilde{u}\)r Astronomie, Universit\(\tilde{a}\)t Wien, T\(\tilde{u}\)rkenschanzstrasse 17, A-1180 Wien, Austria

Received October 15, 1999

**Abstract.** Theoretical calculations indicate that the massive pulsating white dwarf BPM 37093 has a crystallized interior (Winget et al. 1997, Kanaan 1996, Montgomery 1998). Crystallization was predicted theoretically about 40 years ago (Abrisokov 1961, Kirshnitz 1960; Salpeter 1961), but in spite of its importance in astrophysics, there is no direct observational evidence of the theory. Uncertainties in the nature and extent of crystallization, as well as its associated effects, are the largest sources of uncertainties in calculating the ages of the coolest white dwarf stars – important chronometers for the Galactic disk. The Whole Earth Telescope and the Hubble Space Telescope simultaneously observed BPM 37093 in April 1999 in hopes of using asteroseismology to measure its crystallized massfraction. The first step is correct mode identification, principally the spherical harmonic index  $\ell$ . Kanaan et al. (1999) explain the attempt to identify the modes from only the optical WET data, using mainly the periods of the modes. Here we present our preliminary results of applying the Robinson et al. (1995)  $\ell$  identification method which uses a comparison of amplitudes of the modes in the UV and in the optical spectrum.

**Key words:** stars: interiors, white dwarfs, oscillations, individual: BPM 37093, ZZ Ceti

### 1. INTRODUCTION

Kanaan et al. (1992) discovered BPM 37093 as a hydrogen atmosphere white dwarf pulsator (DAV). According to Bergeron et al. (1995), BPM 37093 has a mass of  $M = 1.09 M_{\odot}$ . Koester and Allard's (2000) estimates using IUE spectra are  $T_{\text{eff}} = 11520 \,\text{K}$ ,  $\log q = 8.67, M = 1.03 M_{\odot}$ . Either mass estimate makes BPM 37093 the most massive white dwarf pulsator we currently know. Winget et al. (1997) predicted from the theoretical calculations that this massive DAV star should have a crystallized core. The non-radial g-modes we observe in the pulsating white dwarfs involve predominantly horizontal motions of the material. In our models, the crystallized part of the stellar model cannot sustain shear motions, and this excludes non-radial q-modes. The modes have all their nodes in the non-crystallized part of the model, resulting in modes with longer periods and larger period spacing than they would have in noncrystallized models. Detailed calculations suggest that we should be able to observe this effect (Winget et al. 1997, Montgomery 1998, Montgomery & Winget 1999). If we find observational evidence of crystallization inside BPM 37093, it will be the first such discovery.

Correct mode identification is the key to success in asteroseis-mology. Kanaan et al. (2000) show what they have learned from the Whole Earth Telescope (WET) data gathered in April 1999. The number of modes we observed in BPM 37093 is small, about four modes or so during the WET run. It is therefore difficult to do a unique mode identification using the WET data alone. Considering the scientific importance of detecting crystallization in the stellar interior, we were granted time on the Hubble Space Telescope (HST) to apply a mode identification technique that supplements the standard WET technique.

### 2. LIMB DARKENING METHODS

Robinson et al. (1995) were the first to apply the mode identification method hereafter called "The limb darkening method" to

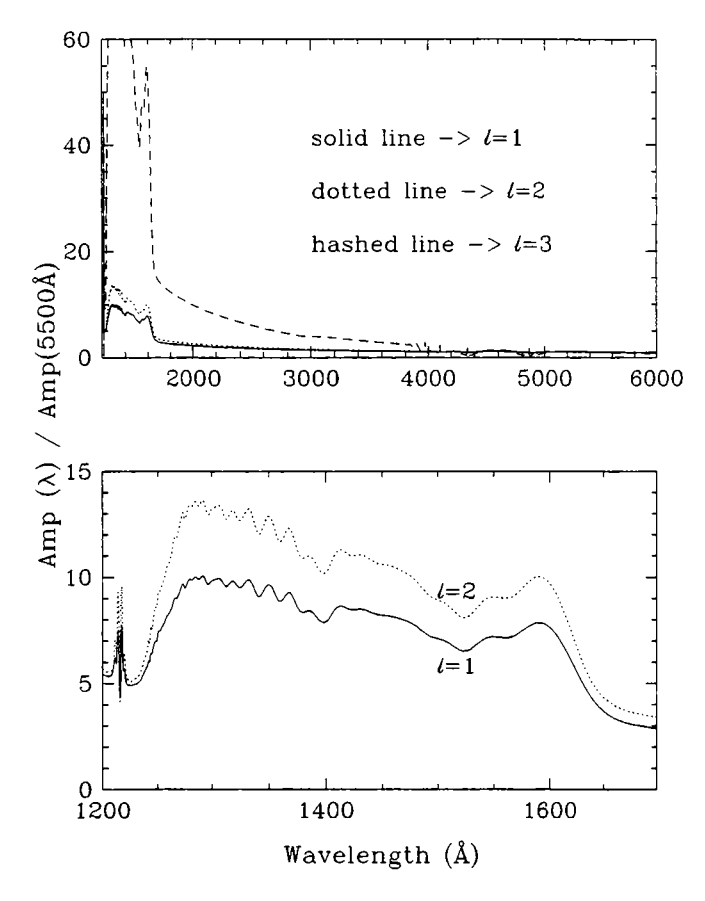


**Fig. 1.** Koester's  $11\,500\,\mathrm{K}\,\log g = 8.75\,\mathrm{model}$ . The x-axis shows wavelength and the y-axis shows the amplitude relative to that at  $5500\,\mathrm{Å}$ .

G 117-B15A, another DAV star. Due to geometric cancellation of the alternating bright and dim patches on the surface of the star and to limb darkening, modes with different  $\ell$  have different amplitudes in the UV compared to those in the optical. Fig. 1 shows the results of theoretical calculations using Koester's state-of-the-art model atmospheres. In this Figure, the amplitudes are normalized to unity at 5500 Å. Regardless of the pulsation modes, real amplitudes and periods, for a given temperature and surface gravity of the model – the amplitude ratio, Amp ( $\lambda$ )/Amp (5500 Å), is a function of the mode  $\ell$  value only. To make use of this result, we need good measurements of amplitudes in both the UV and the optical. The greatest advantage of this method is that the number of modes observed is not impor-

tant. We can determine the  $\ell$  value for a star with a single mode. In the traditional WET approach, we need many observed modes, so we can look for the telltale pattern of equal frequency multiplet splits and equal period spacings. As most white dwarf pulsators do not have the hundreds of modes observed in PG 1159 (Winget et al. 1991) and GD 358 (Winget et al. 1994), this technique may be our best hope of mode identification in the future.

As Kepler (2000) described at this meeting, this method works best with simultaneous coverage in the UV and the optical and accurate period determinations from the optical data. The HST's low orbit and detector constraints make it impossible to get long continuous data sets necessary to measure periods of the modes accurately. Therefore, we need to supplement the HST data with the WET and/or extensive single site data (if the star pulsation modes can be resolved from a single site). Simultaneous data taken in both wavelength regions are vital for pulsators showing any changes in amplitudes. Since our understanding of the pulsation amplitude limiting mechanism is very poor, it is important to have simultaneous data just in case the star shows amplitude modulation during the time of the UV observation even for pulsators previously observed to have constant amplitudes. Since we already knew that BPM 37093 shows amplitude modulation within time scales of hours and days (Kanaan 1996), the coordinated observations between the HST and the WET were essential for these measurements.

The method we normally use to identify modes with extensive optical data, such as WET data, has not been tested against the limb darkening method to see if they both give the same results. Fortunately, this situation will be solved shortly by the planned HST and ground based observations of GD 358, the DBV successfully solved by the WET (Winget et al. 1994) in spring of 2000. Winget et al. (1994) identified all modes observed as  $\ell=1$  modes. We will apply the limb darkening method to GD 358 to see if the same result is got.

## 3. UV OBSERVATIONS BY THE HST

We used the Space Telescope Imaging Spectrograph (STIS) on board of the HST with FUV-MAMA detector, the G140L grating and the  $52 \times 0.5$  slit in TIME-TAG mode. This set up records the position and time of photons as they hit the detector, and the wavelength of a given photon being calculated by the position where it was detected. For our observation, we used the G140L since its spectral

window has the greatest overlap with the wavelength region of the greatest sensitivity for measuring  $\ell$ -values, as seen from the model calculation in Fig. 1. We used the  $52\times0.5$  slit to get as much light as possible from the star without additional complication arising from flatfielding. Flatfielding is done by illuminating the entire slit. But as a star is a point source and does not illuminate the whole slit, the flat field taken in this way is not appropriate for data taken using a larger slit than this. Using the  $52\times0.5$  slit avoids this problem without losing too much light from the target. We split the 7 orbits we had for our scientific observation into two visits, one 3-orbit observation and one 4-orbit observation. Our instrument setup could not to be used for more than four orbits continuously at any time, and two visits must be separated for at least one day. These constraints come from the very sensitive nature of the detector and the limited capability to record the data on board of the HST.

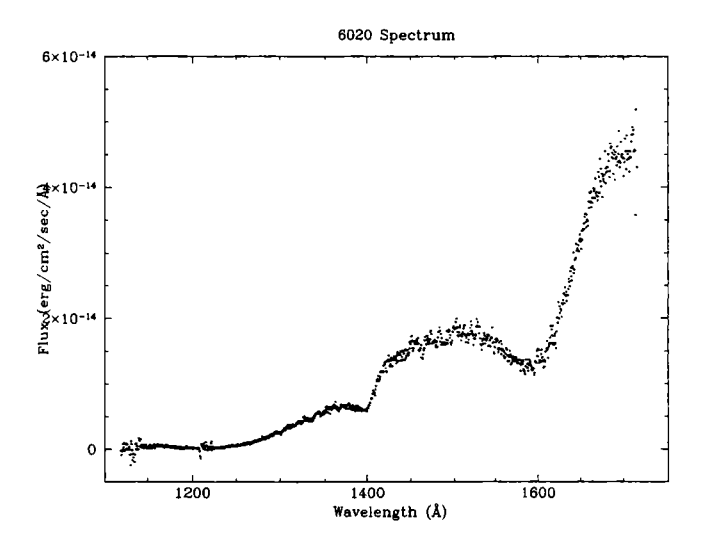


**Fig. 2.** BPM 37093 time averaged spectrum. Note the 1400 Å and 1600 Å quasi-molecular features.

Fig. 2 shows the time averaged spectrum of BPM 37093 over one orbit (3000s). In the reduction process, we can bin the data in a time interval of our choice. We used 80s bins to obtain time-series spectra. To make the time-series spectra into light curves, we simply integrated the flux into 100 Å bins. As you can see in the integrated spectrum (Fig. 2), there is not much flux in 1200–1300 Å range. Since

the IRAF routine, that corrects the data for geocoronal lines, is not perfect, you can see some of the data points have negative flux. Therefore we decided not to use the flux below 1300 Å. We integrated the flux from 1300–1400 Å, 1310–1410 Å, 1320–1420 Å and so on up to 1600–1700 Å. This gave us 31 UV lightcurves. Fig. 3 shows 4 of the 31 UV light curves along with the optical data taken from the ground by WET.

## 4. PRELIMINARY RESULTS

We are still analyzing the data. Here we show preliminary results of what we have found so far.

# 4.1. Spectrum and Fourier Transform

Koester has looked at the integrated HST spectrum of BPM 37093 and found that the mass and temperature estimates remain the same from what he concluded from the IUE data (Koester & Allard 2000).

We show the Fourier transforms of the data and the windows in both the UV and the optical in Fig. 4. The amplitudes are clearly larger in the UV than in the optical. The low resolution in the UV is due to constraints from the instrument and the orbit of the HST. The need and importance of having the optical WET data for period determination of the modes are obvious.

# 4.2. Amplitude modulation

During the WET run we noticed that BPM 37093 was showing amplitude modulation. Fig. 5 shows the running Fourier transform of the optical WET data along with the running window. Each panel is a Fourier transform of a 2-day lightcurve. HST observation took place during the 7th and 8th days. As one can see, the window of these days (labeled as Day 7 – 8 in the Figure) is the best among all the running window. This was achieved thanks to good weather in the Southern hemisphere, and our plan of having the HST observations when the largest number of ground-based telescopes where observing BPM 37093. From Fig. 5, it looks as if the power is moving from the 512s mode to the longer period modes where we saw power during XCOV 16 (1998). As a comparison, we show the Fourier transform from Spring 1998 as well as this WET run (April 1999) in Fig. 6.

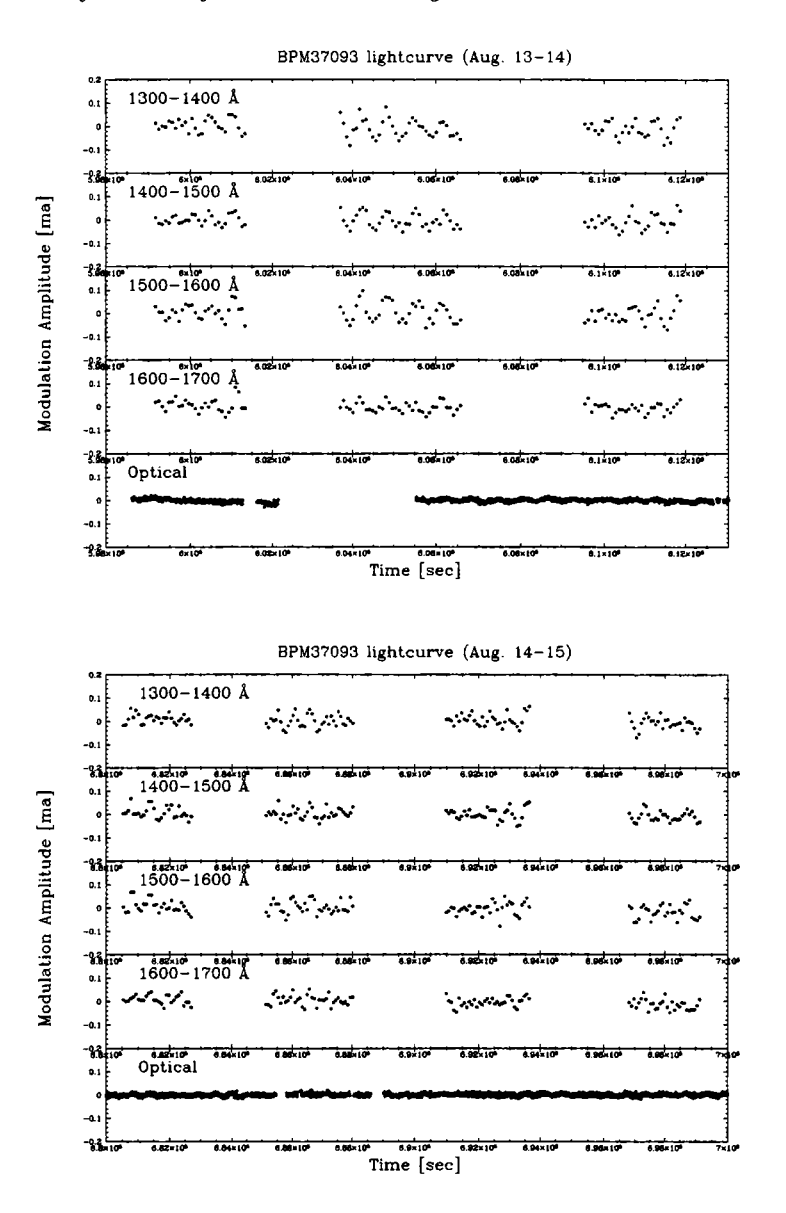


Fig. 3. BPM 37093 lightcurve in the UV and the optical. The top panel shows the lightcurve during the first visit and the bottom panel shows the light curve during the second visit. The vertical scale is the same for both panels. The amplitude is much higher in the UV, which is exactly what models show in Fig. 1. The density of points in the optical data is much higher because they were integrated for each 10 s, while the UV data were integrated over 80 s.

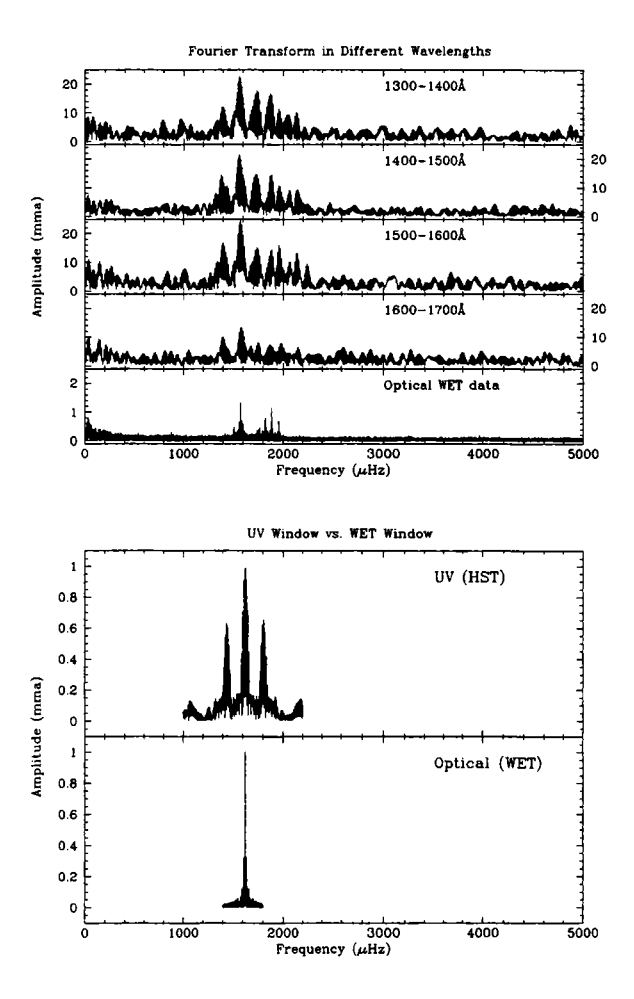


Fig. 4. Top half: Fourier Transform of the data in the UV and optical. All panels have the same vertical scale. Bottom half: the window in the UV and optical. We had a total of 7 orbits of observations with the HST. Due to the low orbit of HST, we can observe BPM 37093 only half of the time during each orbit. The WET window shows how superb a job we can do in determining the periods of the modes in the optical, compared to the HST data.

In Fig. 7, we show how the amplitudes of the four modes (633 s, 531 s, 549 s and 511 s) changed during the WET run. Each point was estimated using a 2-day light curve, simultaneously fitting the 4 modes with periods obtained from the total WET data, with the first point using Day 1-2 data, second point using Day 2-3 data and so

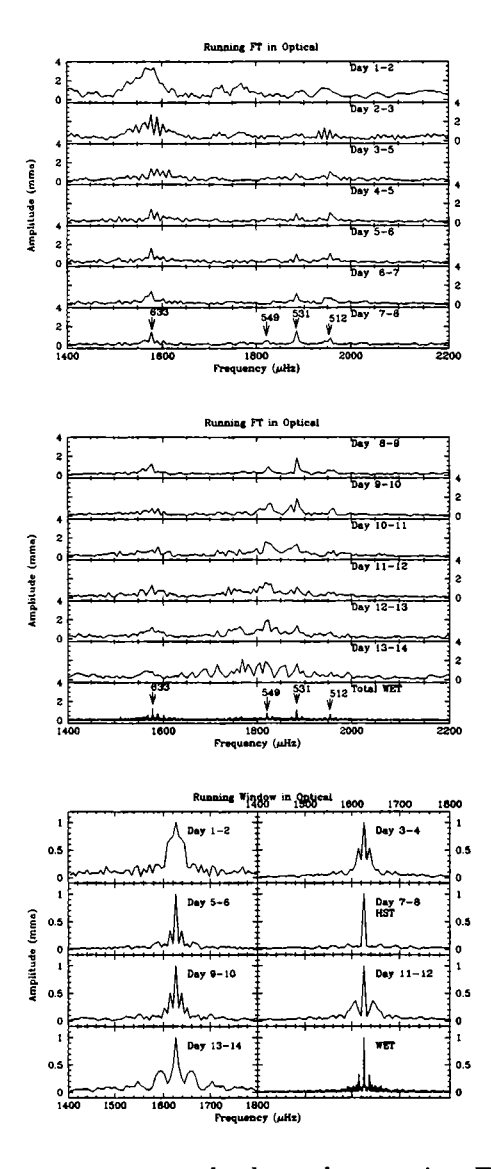


Fig. 5. The two upper panels show the running Fourier Transforms of the 2-day optical lightcurve. One can see how the power spectrum changes during the WET run. Each panel is labeled by the days of the light curve used to produce the Fourier Transforms. For instance, Day 1-2 means the data from the 1st and 2nd day of the WET run. The panel shows Day 7-8 which overlaps with the HST observation, and we labeled the modes by their periods. The Fourier Transform of the total WET data is shown at the bottom of the second panel. The third panel shows the corresponding spectral windows.

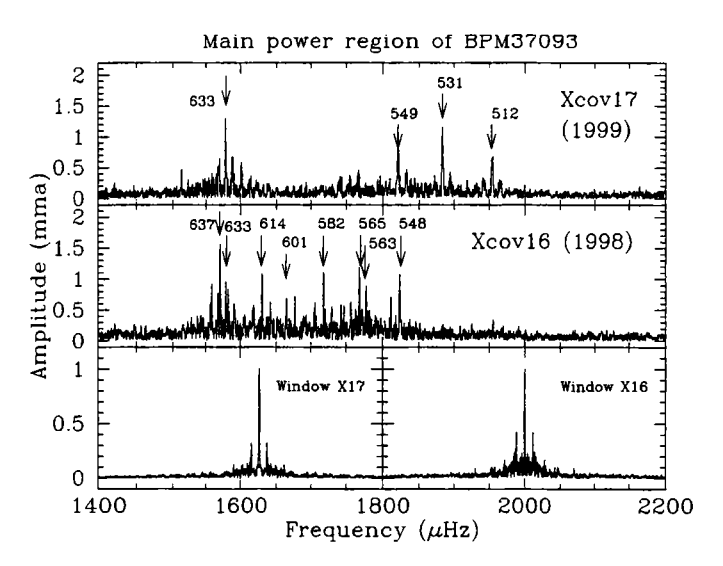


Fig. 6. The Fourier Transform from two WET runs. Comparing of the running FT and this Figure, it looks like during the 1999 WET run (XCOV 17) the power was moving toward the region where the power was located in 1998 (XCOV 16).

on. The  $549\,\mathrm{s}$  mode which was barely present at the beginning of the run, started growing with time and became the highest amplitude mode by the end of the WET run. Meanwhile, the phases of the modes seemed to stay stable (Fig. 8). The first point (the phase of Day 1-2) in Fig. 8 deviates from the calculated phase but it can be accounted for by the poor data quality, since we do not have much data in those two days. The stability of the phases also shows that the changes we see in the modes are truly amplitude modulations, not beating, and the assumption that the periods and the phases of the modes stay constant during the WET run is reasonable.

# 4.3. Mode identification

The limb darkening method requires accurate measurements of the mode amplitudes. If the amplitudes are changing over time, we must measure the amplitudes estimated simultaneously in both UV and optical to obtain the  $\ell$ -value of the modes. We measured the UV amplitude from the HST lightcurves and used the Day 7–8 lightcurve

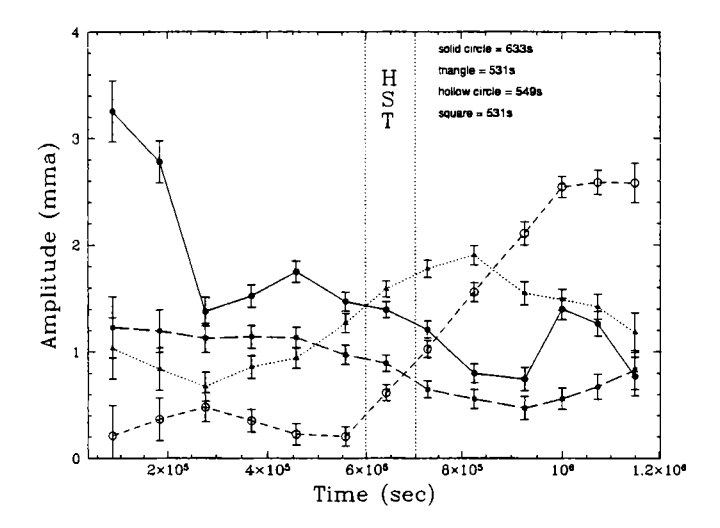


Fig. 7. Amplitude modulation during the WET run. The solid dots are for the 633s mode, with the triangle for the 531s mode, the square for 512 sec, and hollow circle for the 549s mode. The start of the first visit and the end of the second visit of HST observations are shown by the vertical dotted lines.

for the optical amplitudes. The top panel of Fig. 9 shows the model calculation for Koester's  $T_{\rm eff}=11\,500\,{\rm K},\,\log g=8.75$  model. Since his estimates on BPM 37093 are  $T_{\rm eff}=11\,520\,{\rm K},$  and  $\log g=8.67$  (Koester & Allard 2000), this model does not have exactly the same physical parameters, but it is the closest one we have in hand.

If the observed modes all have the same  $\ell$ -value, then they should have the same wavelength dependence in Fig. 9. The first thing we see is that none of the modes are  $\ell=3$ . Among the four modes, the shape of the 531s curve looks very similar to that of the model  $\ell=1$  mode. The curves of 633s and 512s modes look almost parallel to each other and don't fit neither the model for  $\ell=1$  nor  $\ell=2$  curve very well. The curve of the 549s mode is very noisy. As we saw in Fig. 7, the amplitude of the 549s mode was just starting to grow around the time of the HST observation. The amplitude is still the smallest among the four modes. In Fig. 10, we show the phases of the four modes in the UV compared to the phases estimated using the optical data around the HST observation (Day 7-8 light curve).

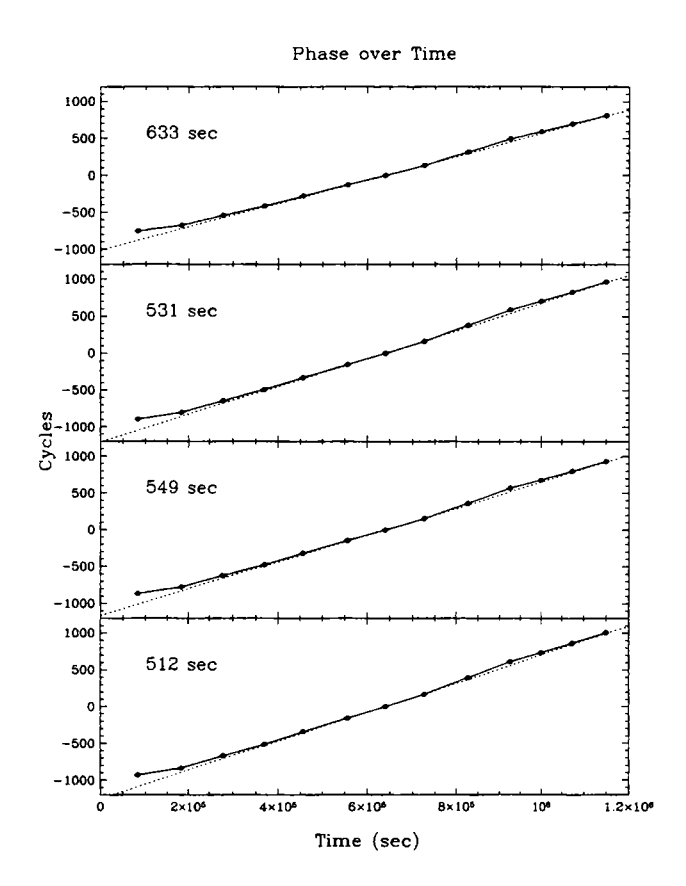


Fig. 8. Phases of four modes over time in the optical. The y-axis shows the number of cycles counted from the middle of the run (run 7-8) when the coverage was the best. Each point was estimated using a 2-day light curve of optical data, and the dotted line shows the calculated phase assuming constant phase over time.

Error bars show the formal errors estimated from the least square fitting program; therefore they are much smaller than the true error. It is seen that the 549s mode's phase has much larger error bars and scatter compared to the other three modes, indicating that the estimates of the UV amplitude of this mode are of lower accuracy. A successful mode identification with the data on the 549s mode seems very unlikely. The other three modes have similar phases in all UV wavelengths, but are slightly offset from that of the optical.

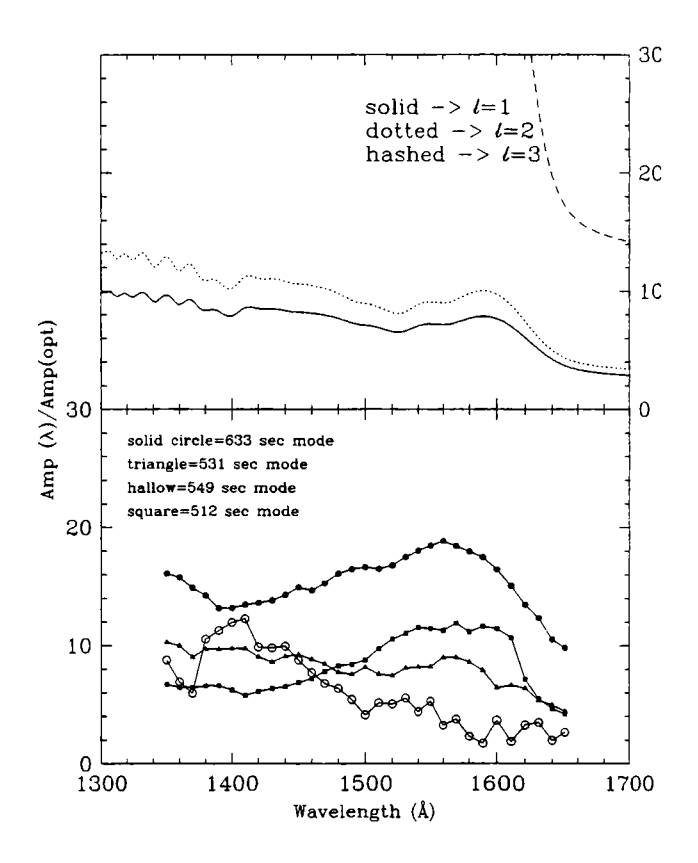
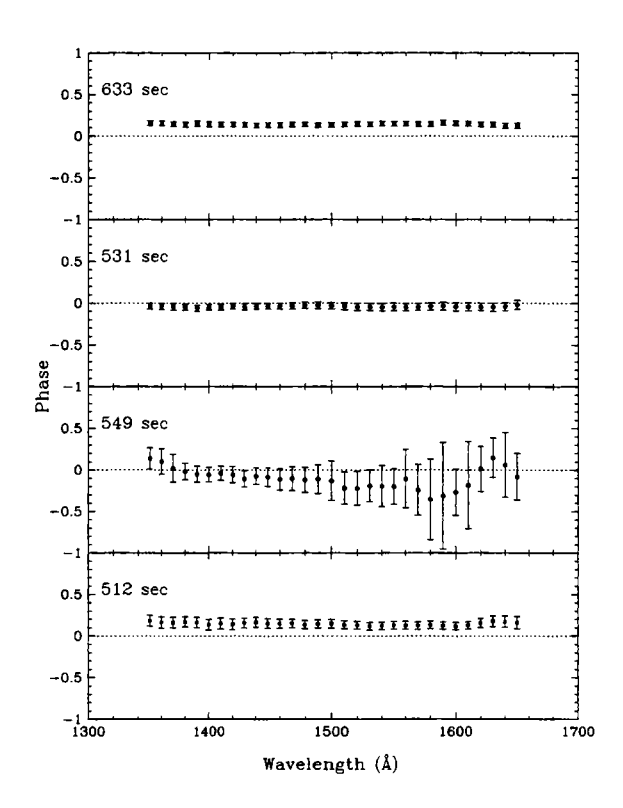


Fig. 9. The UV amplitude normalized by the optical amplitude. The top panel shows the calculated amplitude ratio using Koester's model with  $T_{\rm eff}=11\,500\,{\rm K}$  and  $\log g=8.75$ . The solid line is for the model  $\ell=1$  mode, the dotted line is for the model  $\ell=2$  mode and dashed line is for the model  $\ell=3$  mode. The bottom panel shows the data on all observed 4 modes.

According to Robinson, Kepler & Nather (1982), the modes should have the same phase at all wavelengths if nonadiabatic effects are not important. Perhaps Fig. 9 indicates that the UV data, being short and not continuous, are not good enough to estimate the phase accurately. In our amplitude estimates, we should use not only the fixed periods obtained from the total WET data, but also use the fixed phase from the WET data.



**Fig. 10.** Relative (UV to optical) phases of 4 modes vs. wavelength. When the phase is equal to zero, the UV is in phase with the optical data. When it is  $\pm 0.5$ , it means that the UV phase is out of phase ( $\pm \pi$ ) with the optical. The phases of 633 s, 531 s, 549 s modes appear in phase in phase within the UV, but have offset from the optical phase.

#### 5. CONCLUSION AND FUTURE WORK

We are still analyzing the data, and at this point we can conclude that the four modes we observed are not  $\ell \geq 3$ , but we cannot give definite mode identifications. Fig. 9 shows that the mode identification is not as clear-cut as we would have like it to be. One thing we will try is to use the fixed optical periods and phases of the modes for our UV amplitude estimates. We also have another approach to the mode identification we would like to try. The essence of the limb darkening method is that the pulsation amplitude in one wavelength

differs only by a constant factor from the amplitude in another wavelength. This holds as long as the pulsation modes we observe can be described by spherical harmonics, limb darkening and a good atmosphere model describing the white dwarf atmosphere. All three assumptions should be valid for nonradial q-modes observed in white dwarfs. Another way of stating is that the light curve taken in one wavelength differs by a constant factor from the lightcurve taken in another wavelength if all modes in the white dwarf has the same  $\ell$ -value. If all modes in BPM 37093 are of the same  $\ell$  value, the light curve in one of the UV wavelength bin is by a constant factor the lightcurve in the optical. Instead of estimating the amplitudes of each mode, we can use the light curves to obtain the factors of light curve relations. We would like to see if this approach will work on BPM 37093, but before applying it to BPM 37093, we will first try it on GD 358, which we know from Winget et al. (1994) has only  $\ell = 1$ , and we already have its UV data at hand from the HST observations in 1996. As Kepler discussed in this meeting (Kepler et al. 2000), at the time of the GD 358 observations, the HST had the Faint Object Spectrograph (FOS) on board. This instrument, in the setting we used, has a Zeroth order reflection which has an effective wavelength similar to U band (3400 Å). The Zeroth order data and the the normal UV data are taken simultaneously, and are therefore an ideal test how this integral method of mode identification works.

ACKNOWLEDGMENTS. Support of this work was provided by NASA through grant number GO-07301.01-97A from Space Telescope Science Institute, which is operated by the Association of Universities for Research in Astronomy, Inc., under NASA contract NAS5-26555. This work was also supported in part by National Science Foundation Grant No. AST-9315461.

### REFERENCES

Abrisokov A. 1961, Soviet Phys.-JETP, 12, 1254

Bergeron P. et al. 1995, ApJ, 258, 449

Kanaan A. et al. 1992, ApJ, 390, L89

Kanaan A. 1996, PhD Thesis, University of Texas at Austin

Kanaan A., A. Nitta-Kleinman, D. E. Winget et al. 2000, in The Fifth WET Workshop Proceedings, eds. E. G. Meištas & G. Vauclair, Baltic Astronomy, 9, 87 Kepler S. O., Robinson E. L., Koester D. et al. 2000, in The Fifth WET Workshop Proceedings, eds. E. G. Meištas & G. Vauclair, Baltic Astronomy, 9, 59

Koester D., Allard N. F. 2000, in *The Fifth WET Workshop Proceedings*, eds. E. G. Meištas & G. Vauclair, Baltic Astronomy, 9, 113

Kirshnitz D. A. 1960, Soviet Phys.-JETP, 11, 365

Montgomery M. H. 1998, PhD Thesis, University of Texas at Austin

Montgomery M. H., Winget D. E. 1999, ApJ, 526, 976

Robinson E. L., Kepler S. O., Nather R. E. 1982, ApJ, 259, 219

Robinson E. L. et al. 1995, ApJ, 438, 908

Salpeter E. 1961, ApJ, 134, 669

Winget D. E. et al. 1991, ApJ, 378, 326

Winget D. E. et al. 1994, ApJ, 430, 839

Winget D. E. et al. 1997, ApJ, 487, L191